CELL CYCLE
2020, VOL. 19, NO. 20, 2600–2610
https://doi.org/10.1080/15384101.2020.1810401

Taylor & Francis
Taylor & Francis Group

RESEARCH PAPER

Melatonin inhibits oxalate-induced endoplasmic reticulum stress and apoptosis in HK-2 cells by activating the AMPK pathway

Qianlin Song[a], Ziqi He[a], Bin Li[a], Junwei Liu[a], Lang Liu[a], Wenbiao Liao[a], Yunhe Xiong[a], Chao Song[a], Sixing Yang[a], and Yunlong Liu[b]

[a]Department of Urology, Renmin Hospital of Wuhan University, Wuhan, People's Republic of China; [b]Department of Urology, The First Affiliated Hospital of Zhengzhou University, Zhengzhou, Henan, People's Republic of China

ABSTRACT

Background: Deposition of various crystal and organic substances in the kidney can lead to kidney stone formation. Melatonin is an effective endogenous antioxidant that can prevent crystalluria and kidney damage due to crystal formation and aggregation. In this study, we investigated the mechanism by which melatonin inhibits endoplasmic reticulum (ER) stress and apoptosis.

Methods: We treated HK-2 cells with oxalate to establish an *in vitro* kidney stone model, and treated these cells with different concentrations of melatonin (0, 5, 10, 20 μmol/L) and the AMP-activated protein kinase (AMPK) inhibitor Compound C. We measured levels of stress response markers including reactive oxygen species (ROS), lactate dehydrogenase (LDH), glutathione (GSH), superoxide dismutase (SOD), malondialdehyde (MDA), catalase (CAT), and factors in the stress response pathway, such as ATF6, GRP78, DDIT3, PERK, p-PERK, IRE1, p-IRE1, XBP1s, AMPK, and p-AMPK, using real time-PCR, western blot, and immunofluorescence analyzes. We measured mitochondrial membrane potential and caspases-3 activity using the CCK8, enzyme-linked immunosorbent, and flow cytometry assays to assess HK-2 cell viability and apoptosis.

Results: Melatonin improved the total antioxidant capacity (T-AOC) of the HK-2 cells, as evidenced by the dose-dependent reduction in apoptosis, ROS levels, and protein expression of ATF6, GRP78, DDIT3, p-PERK, p-IRE1, XBP1s, caspase-12, cleaved caspase-3 and cleaved caspase-9. Addition of the AMPK inhibitor, Compound C, partially reversed the protective effect of melatonin.

Conclusion: Our study revealed that the protective effects of melatonin on oxalate-induced ER stress and apoptosis is partly dependent on AMPK activation in HK-2 cells. These findings provide insight into the prevention and treatment of kidney stones.

ARTICLE HISTORY
Received 17 March 2020
Revised 2 July 2020
Accepted 10 August 2020

KEYWORDS
Kidney stone; melatonin; AMPK; oxalate; endoplasmic reticulum stress; apoptosis

Introduction

Kidney stones, or renal calculi, are a common urological disease that has a global prevalence rate of 1.7%, with a higher frequency in males than in females. The recurrence rate within 5 years post-surgery is approximately 50% [1,2]. A hectic lifestyle, irregular diet, and global warming can contribute to the occurrence of kidney stones [3]. High prevalence and recurrence of kidney stone formation, high patient volume, and treatment cost pose a heavy burden for patients and society as a whole [4]. Hyperoxaluria, which arises from hyperoxalate-induced damage of renal tubular epithelial cells, is an important risk factor for urinary calculi formation [5,6]. Long-term accumulation of oxalate can induce endoplasmic reticulum (ER) stress in renal tubular epithelial cells and lead to excessive reactive oxygen species (ROS) production [7,8]. Increased ROS levels can lead to degeneration, apoptosis, and necrosis of renal tubular epithelial cells, leading to basement membrane exposure, thereby triggering crystal nucleation, aggregation, and growth of kidney stones [9,10].

Melatonin is a hormone secreted primarily by the pineal gland in most organisms, but can also be produced in the brain, gastrointestinal tract, kidney, pancreas, spleen, immune cells, and reproductive tract [11–13]. Melatonin acts as an endogenous antioxidant and can directly or indirectly scavenge free radicals and reduce ROS levels, thus reducing oxidative stress [14]. Moreover, melatonin has been shown to prevent crystalluria and kidney damage that arise from crystal formation

CONTACT Sixing Yang sxyang2004@163.com Yunlong Liu asphds@163.com
This article has been republished with minor changes. These changes do not impact the academic content of the article.

and aggregation [15]. AMP-activated protein kinase (AMPK) activation was found to be associated with melatonin's antioxidant effect in reducing blood lipids and vascular calcification [16,17]. AMPK plays a key role in regulating cellular energy, mitochondrial function, and ER stress *in vivo* [18], as well as in cell growth, differentiation, autophagy, and metabolism [19,20]. Elevated oxalate concentrations can reduce intracellular ATP levels [21], which prevents AMPK activation [22]. Moreover, melatonin-induced activation of AMPK and inhibition of ER stress have been demonstrated in inflammatory bodies and hypoxia-reoxygenation injury [23,24].

However, it remains unclear if AMPK is involved in melatonin's effect on oxalate-induced ER stress and apoptosis. Thus, we designed this study to clarify the underlying signal transduction mechanism of melatonin on oxalate-induced ER stress using human proximal tubular (HK-2) cells. Our findings provide new insight into the prevention and treatment of kidney stones.

Materials and methods

Cell culture and grouping

HK-2 cells (Cell Bank of the Chinese Academy of Sciences, Shanghai, China) were cultured in DMEM/F12 complete medium (DMEM/F12 basic medium (Gibco, USA)) with 10% fetal bovine serum (Biological Industries, Israel) and 100 μg/ml penicillin/streptomycin (Beyotime, China) in a humidified incubator at 37°C and 5% CO_2. The culture medium was refreshed once a day and cells were passaged at a 1:2 ratio every three days. When the cells reached 70–80% confluency, the medium was refreshed and the cells were divided into five treatment groups. Melatonin was dissolved in DMSO to obtain an initial stock concentration of 50 mM, which was then diluted with basic medium to make 5 μM, 10 μM, and 20 μM dilution stocks for use. The final concentrations of DMSO in these dilution stocks were 0.01%, 0.02%, and 0.04%, respectively. Since DMSO concentrations below 0.1% are minimally toxic [25], there were no concerns of potential DMSO-mediated toxicity in our cells. The negative control "NC" group was cultured without treatment for 12 h; the "Ox group" was treated with 4 mmol/L of oxalate (Sigma, Germany) for 12 h; and the "Ox + MLT group" was treated with 4 mmol/L oxalate + melatonin (MLT) (5, 10, and 20 μmol/L) (Selleck, USA) for 12 h. These five treatment groups were used to determine the effects of melatonin on ER stress and apoptosis. To determine the effect of blocking the AMPK pathway in the melatonin response, we treated HK-2 cells with 4 mmol/L Ox + 10 μmol/L MLT + 5 μmol/L of the AMPK inhibitor Compound C 2HCl (Selleck, USA) (Ox + MLT + Cpd C 2HCl group) for 12 h. Compound C is an effective, reversible, and selective AMPK inhibitor [26]. Compound C 2HCl was dissolved in sterilized deionized water to obtain an initial stock concentration of 10 mM, which was then diluted with basic medium to make 10 μM dilution stocks for use.

Cell viability assay

Cell viability was determined using the CCK8 assay (Dojindo, Japan). HK-2 cells were cultured in a 96-well plate and subjected to their respective interventions. Next, 100 μl of the CCK8 solution (CCK8 10 μl + basal medium 90 μl) was added to each well, and the cells were incubated for 2 h at 37°C. Absorbance was measured at 450 nm with a microplate reader (Perkin Elmer, USA).

Lactate dehydrogenase (LDH) assay

The LDH assay was performed on HK-2 cells in the respective treatment groups. The LDH release reagent (10% of the original culture volume) in the Cytotoxicity Assay Kit (Beyotime, China) was incubated with the HK-2 cells in a control well of the 96-well plate at 37°C for 1 h. The 96-well plate was then centrifuged at 400 rpm for 5 min. Next, 120 μl of the supernatant from all wells was transferred to a new 96-well plate and incubated with 60 μl of LDH detection working solution at room temperature (25°C) in the dark for 30 min before measuring the absorbance at 490 nm with a microplate reader.

Cell biochemical indicators

We measured the biochemical indicators glutathione (GSH), superoxide dismutase (SOD),

malondialdehyde (MDA), catalase (CAT), and total antioxidant capacity (T-AOC) using the following kits according to the manufacturers' instructions: GSH (Njjcbio, A006-2-1), SOD (Njjcbio, A001-3-2), MDA (Njjcbio, A003-4-1), CAT (Solarbio, BC0205), and T-AOC (Njjcbio, A015-2-1). Absorbance was measured with a microplate reader at 405 nm (GSH), 450 nm (SOD), 530 nm (MDA), 240 nm (CAT), and 405 nm (T-AOC).

ROS measurement

HK-2 cells in the respective treatment groups were washed twice with phosphate buffered saline (PBS) and then trypsinized (EDTA-free) to obtain cell suspensions. Cell suspensions for each treatment group were collected, centrifuged for 5 min, and incubated with 10 μmol/L 2,7-Dichlorodihydrofluorescein diacetate (DCFH-DA) (Beyotime, China) for 20 min. The mixture was agitated by inversion every 3–5 min to ensure thorough mixing. Next, the cell suspensions were washed thrice with serum-free cell culture solution, and then resuspended in 500 μl PBS by gentle mixing before ROS levels were measured using a flow cytometer (Becton Dickinson, USA).

Mitochondrial membrane potential

The mitochondrial membrane potential of HK-2 cells cultured in 6-well plates was measured to determine the effect of melatonin treatment on apoptosis. Cell climbing tablets were mixed with 2 ml of diluted JC-1 (5,5,6,6-Tetrachloro-1,1,3,3-tetraethyl-imidacarbocyanine iodide) staining solution (1 ml of serum-free medium + 1 ml JC-1 stain (Beyotime, China)) and incubated for 20 min at 37°C. The staining solution was removed and the cells were washed twice with JC-1 staining buffer (1×) before mounting with Antifade Mounting Medium (containing DAPI) (Beyotime, China). Cells were immediately observed under an automated fluorescence microscope (Olympus, Japan) at 200× magnification. The mean signal intensities of red and green fluorescence were analyzed using ImageJ software (NIH, USA).

The mitochondrial membrane potential in cells treated with the AMPK inhibitor was detected using Mito-Tracker Red chloromethyl-X-rosamine (CMXRos; Beyotime, China). Compound C 2HCl-treated HK-2 cell climbing tablets were incubated with diluted Mito-Tracker Red CMXRos staining solution for 20 min at 37°C. The staining solution was removed and cells were washed once with serum-free medium and PBS before mounting with Antifade Mounting Medium (containing DAPI). Cells were immediately observed under an automated fluorescence microscope at 200× magnification.

Caspase-3 enzyme activity detection

HK-2 cell climbing tablets were incubated with 500 μl of GreenNucTM Caspase-3 Substrate (5 μmol/L; Beyotime, China) for 20 min before mounting with Antifade Mounting Medium (containing DAPI). Cells were visualized and imaged under an automated fluorescence microscope at 200× magnification.

Caspase-3 activity was detected using a caspase-3 enzyme-linked immunosorbent assay (ELISA) assay kit (Cusabio, China). HK-2 cells were washed once with pre-chilled PBS (1X) before collection, followed by incubation at 20°C for 12 h. The cells were centrifuged at 5,000 g for 5 min at 4°C and the supernatant was collected. The supernatant was incubated with 100 μl of the standard sample provided in the kit for 30 min at 37°C, washed three times, incubated with 100 μl HRP-conjugate (1X) for 30 min at 37°C, and then washed five times. The supernatant was next incubated with the TMB substrate (90 μl) for 20 min at 37°C in the dark before 50 ul of stop solution was added. Optical density at 450 nm was immediately measured using a microplate reader.

Flow cytometry

HK-2 cells were trypsinized and pelleted to obtain a cell suspension. The cell suspension was gently mixed with 500 μl Annexin V Binding Buffer (1×) (BD Pharmingen, USA), 5 μl of R-phycoerythrin (PE) Annexin V, and 7-Amino-Actinomycin (7-AAD). The cells were then incubated for 15 min at room temperature (25°C) in the dark

before flow cytometric analysis to measure cell apoptosis.

Real-time RT-PCR

Total RNA extraction was performed using Trizol reagent according to the manufacturer's instructions. Using the NanoDrop™ One (Thermo Fisher Scientific, USA), we determined the RNA concentration and purity of each group using 1 μg/μl with an A260/A280 = 1.8 ~ 2.0. Total RNA was reverse transcribed into cDNA using the PrimeScript™RT reagent kit with gDNAEraser (Perfect Real Time, Takara, Japan). Target gene mRNA expression levels were detected using TB Green® Premix Ex Taq™ II (TliRNaseH Plus, Takara, Japan). To minimize genomic DNA contamination, a 1:20 dilution of total RNA (100 ng total RNA per 20 μl qPCR reaction) was used for qPCR to allow us to obtain enough cDNA and perform a wide range of cDNA dilutions. All qPCR reactions were run in triplicates using probes for the target genes and GAPDH on a BIO-RAD CFX Real-Time PCR System. The relative gene expression level of the target genes was determined using the formula:Ratio = $(1+ E_{target})^{\Delta Ct\ target(control-expt)}$ $/(1+ E_{reference})^{\Delta Ct\ reference(control-expt)}$. The sequences of the primers used for RT-PCR were as follows: DDIT3, forward 5′- GGTATGAGGACCTGCAAGA GGT-3′, reverse 5′- CTTGTGACCTCTGCTGGTTC TG-3′; GRP78, forward 5′- CTGTCCAGGCTGG TGTGCTCT-3′, reverse 5′- CTTGGTAGGCACCAC TGTGTTC-3′; ATF6, forward 5′- CAGACAGTAC CAACGCTTATGCC-3′, reverse 5′- GCAGAACTC CAGGTGCTTGAAG-3′; XBP1s forward 5′- AGTCC GCAGCAGGTGCAG –3′, reverse 5′- CTTCC AGCTTGGCTGATGAC –3′.

Western blot analysis

Total protein was extracted from cell lysates, separated by 10–15% SDS-PAGE, and then transferred onto PVDF membranes (Millipore, USA). Membranes were blocked in 5% skim milk for 1 h, washed three times with Tris buffered saline with Tween 20 (TBST), and then incubated with the following primary antibodies at 4°C for 12 h: ATF6 (Proteintech, China, 24,169-1-AP), GRP78 (Proteintech, 11,587-1-AP), DDIT3 (Proteintech, 15,204-1-AP), caspase-12 (Proteintech, 55,238-1-AP), cleaved caspase-3 (Proteintech, 19,677-1-AP), cleaved caspase-9 (Proteintech, 10,380-1-AP), PERK (Proteintech, 20,582-1-AP), phosphorylated (p)-PERK (Affinity, China, DF7576), IRE1 (Proteintech, 27,528-1-AP), p-IRE1 (Affinity, AF7150), XBP1s (CST, USA, 12,782), AMPK (Proteintech, 66,536-1-Ig), p-AMPK (Affinity, AF3423), and GAPDH (Abcam, UK, ab181602). Blots were incubated with corresponding secondary antibodies (Servicebio, China, GB23303/Proteintech, SA00001-1) for 1 h at room temperature. An enhanced chemiluminescence reagent was added and the membranes were visualized and analyzed using Image J software (NIH, USA).

Immunofluorescence

HK-2 cell climbing tablets were fixed in universal tissue fixation solution (Servicebio, China) for 15 min at room temperature, washed three times with PBS and once with 0.3% Triton-PBS for 10 min at room temperature, and then blocked with 5% bovine serum albumin (BSA) (Servicebio, China) at room temperature for 30 min. Next, the cells were washed twice with PBS and incubated with the respective primary antibodies at 4°C in the dark for 12 h. The cell climbing tables were then washed three times with PBS, incubated with 0.3% Triton-PBS for 10 min at room temperature, washed twice, and then incubated with the corresponding fluorescent secondary antibody (CST, 4412) for 30 min at room temperature in the dark. Finally, the cell climbing tablets were washed three times with PBS, mounted with Antifade Mounting Medium (containing DAPI), enclosed with a cover glass, and placed in the cassette for visualization and imaging under an automated fluorescence microscope at 200× magnification.

Statistical analysis

All data are expressed as mean ± standard error of the mean (SEM) of at least three independent experiments. All statistical analyses were performed using GraphPad Prism software version 7.0. Comparisons between two groups were determined using the Student's t-test, while comparisons between multiple groups were analyzed using

one-way analysis of variance (ANOVA) followed by Tukey's post-hoc tests. P values < 0.05 were considered statistically significant.

Results

Melatonin increases cell viability and improves antioxidant capacity in HK-2 cells

To determine the effects of melatonin on oxalate-induced damage and antioxidant capacity of HK-2 cells, we assessed cell viability using the CCK8 assay and measured the biochemical indicators LDH, MDA, T-AOC, CAT, GSH, and SOD in the NC, Ox, and Ox + MLT groups. Compared with the NC group, the Ox group showed decreased cell viability (Figure 1(a)), decreased T-AOC and intracellular GSH, SOD, and CAT antioxidant levels (Figure 1(dg)), and increased LDH and MDA levels (Figure 1(b,c)). Compared with the Ox group, the Ox + MLT group showed increased cellular viability (Figure 1(a)), increased T-AOC and intracellular GSH, SOD, and CAT antioxidant levels (Figure 1(dg)), and decreased LDH and MDA levels (Figure 1(b,c)). These results suggest that melatonin can dose-dependently affect HK-2 cell viability and antioxidant capacity.

Melatonin can decrease ROS production and apoptosis

To determine the effect of melatonin on ROS production and oxalate-induced apoptosis in HK-2 cells, we performed flow cytometry and immunofluorescence assays in the three treatment groups. Compared with the NC group, the Ox group showed increased ROS production (Figure 2(a)), a higher early and late apoptotic rate (Figure 2(b)), decreased mitochondrial membrane potential (Figure 2(c)), and increased caspase-3 activity (Figure 2(d,e)). Compared with the Ox group, the Ox + MLT group showed decreased ROS production (Figure 2(a)), a decreased early and late apoptotic rate (Figure 2(b)), increased mitochondrial membrane potential (Figure 2(c)), and decreased caspase-3 enzyme activity (Figure 2(d,e)).

Melatonin can reduce ER stress-related protein and mRNA expression levels

ER stress can trigger three apoptosis signaling pathway mediators – PERK, IRE1, and ATF6 – leading to cellular damage [27]. Thus, we performed western blot and RT-PCR analyzes to determine the effect of melatonin on oxalate-induced ER stress response in HK-2 cells. Compared with the NC group, the Ox group showed increased mRNA and protein levels of GRP78, DDIT3, ATF6, and XBP1s (Figure 3(a, b)), as well as increased p-PERK and p-IRE1 protein expression (Figure 3(b)). Compared with the Ox group, the Ox + MLT group showed reduced mRNA levels of GRP78, DDIT3, ATF6, and XBP1s (Figure 3(a)). Moreover, a dose-dependent reduction in protein expression of GRP78, DDIT3, ATF6, p-PERK/PERK, p-IRE1/IRE1 and XBP1s was also observed (Figure 3(b)). These results

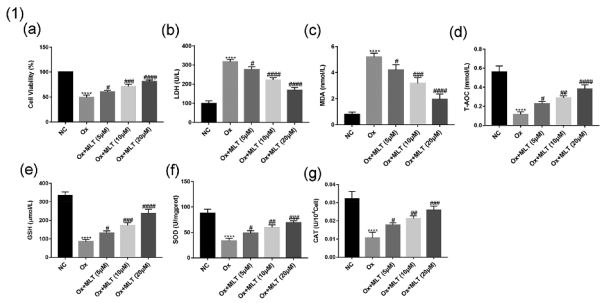

Figure 1. Impact of melatonin on HK-2 cell antioxidant capacity and viability. Cells in each group were treated for 12 h with 4 mmol/L Ox (except the NC group). Comparisons of (a) cell viability, (b) LDH content, (c) MDA content, (d) T-AOC content, (e) GSH content, (f) SOD content, and (g) CAT content. Data are presented as the means ± SEM from three independent experiments. *P < 0.05, **P < 0.01, ***P < 0.001,****P < 0.0001, versus the NC group; #P < 0.05, ##P < 0.01, ###P < 0.001, ####P < 0.0001, versus the Ox group.

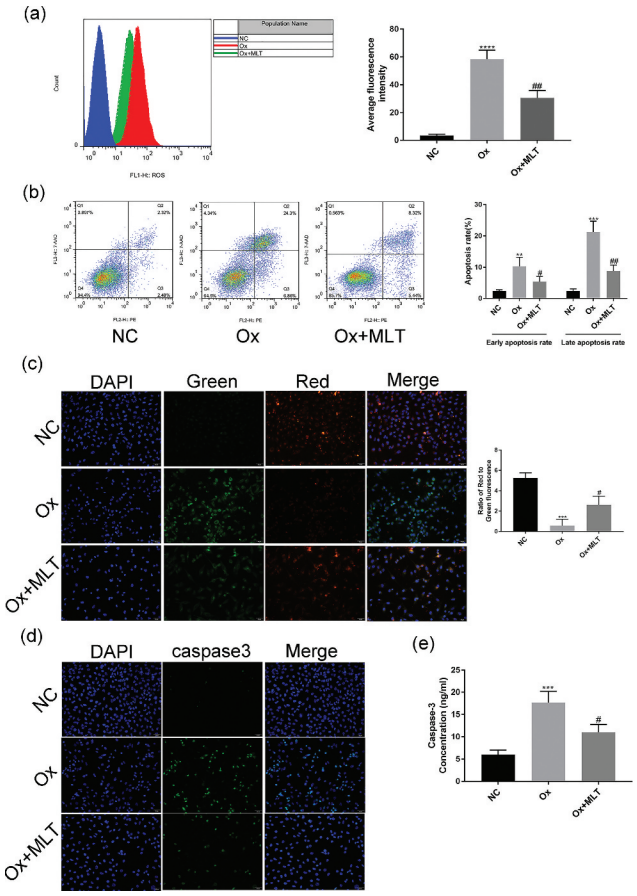

Figure 2. Impact of melatonin on ROS production and apoptosis in HK-2 cells. Cells in the respective groups were treated for 12 h with 4 mmol/L Ox (except the NC group) and 10 μmol/L MLT (Ox + MLT group only). Flow cytometry profiles and corresponding histograms showing (a) ROS levels and (b) early and late apoptotic rate in three treatment groups. Immunofluorescence images showing (c) mitochondrial membrane potential and (d) caspase-3 activity (200× magnification), and (e) histogram of ELISA showing caspase-3 activity. The reduction in mitochondrial membrane potential (transition from red to green fluorescence) is a sign of early apoptosis. Stronger green fluorescence indicates higher caspase-3 activity. Data are presented as the means ± SEM from three independent experiments. *P < 0.05, **P < 0.01, ***P < 0.001, ****P < 0.0001 versus the NC group; #P < 0.05, ##P < 0.01, ###P < 0.001, ####P < 0.0001 versus the Ox group.

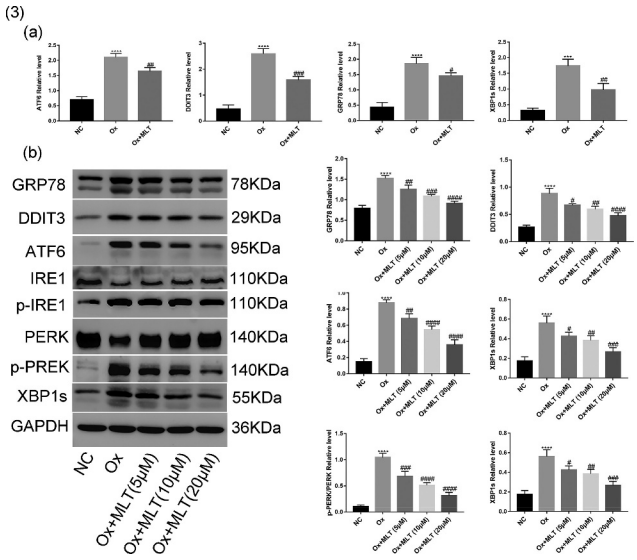

Figure 3. Impact of melatonin on ER stress-related protein and mRNA levels. Cells in each group were treated for 12 h with 4 mmol/L Ox (except the NC group) and 10 μmol/L MLT (except NC and Ox groups). (a) RT-PCR histograms of mRNA levels of DDIT3, GRP78, ATF6, and XBP1s relative to GAPDH. (b) Western blot and corresponding histograms of DDIT3, GRP78, ATF6, PERK, p-PERK, IRE1, p-IRE1, and XBP1s protein expression relative to GAPDH. Data are presented as the mean ± SEM from three experiments. *P < 0.05, **P < 0.01, ***P < 0.001, ****P < 0.0001 versus the NC group; #P < 0.05, ##P < 0.01, ###P < 0.001, ####P < 0.0001 versus the Ox group.

suggest that melatonin can dose-dependently reduce oxalate-induced ER stress.

Melatonin can induce AMPK activation and decrease expression of apoptotic proteins

Western blot analysis was used to verify the effect of melatonin on protein expression of apoptotic and AMPK proteins. Compared with the NC group, the Ox group showed increased expression of caspase-12, cleaved caspase-3, and cleaved caspase-9, decreased expression of p-AMPK/AMPK (Figure 4). Compared with the Ox group, the Ox + MLT group showed decreased expression of caspase-12, cleaved caspase-3, and cleaved caspase-9, increased expression of p-AMPK/AMPK (Figure 4). These results suggest that oxalate treatment inhibits AMPK in HK-2 cells, while melatonin dose-dependently induces AMPK activation and decreases the expression of apoptotic proteins.

AMPK inhibition increases HK-2 cell apoptosis and decreases mitochondrial membrane potential

We used the AMPK inhibitor Compound C 2HCl to determine if AMPK is involved in melatonin's effect on apoptosis. Compared with the Ox + MLT group, the Ox + MLT + Cpd C 2HCl group showed increased HK-2 cell early and late apoptosis (Figure 5(a)), and decreased mitochondrial membrane potential (Figure 5(b,c)) and caspase-3 activity (Figure 5(d)). This suggests that

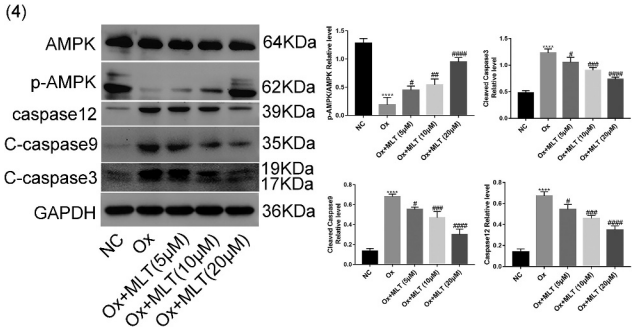

Figure 4. Impact of melatonin on expression of AMPK and apoptotic proteins. Cells in each group were treated with 4 mmol/L of Ox for 12 h (except the NC group). Western blot and corresponding histograms of protein expression levels of caspase-12, cleaved caspase-3, cleaved caspase-9, p-AMPK, and AMPK relative to GAPDH. Data are presented as the mean ± SEM from three independent experiments. *P < 0.05, **P < 0.01, ***P < 0.001, ****P < 0.0001 versus the NC group; #P < 0.05, ##P < 0.01, ###P < 0.001, ####P < 0.0001 versus the Ox group; ns: not significant.

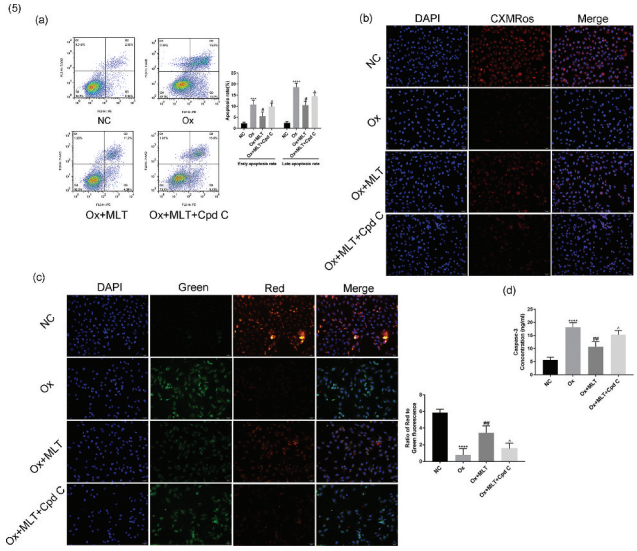

Figure 5. Effect of AMPK inhibition on melatonin-mediated regulation of apoptosis and mitochondrial membrane potential. Cells in each group were treated for 12 h with 4 mmol/L Ox, 10 μmol/L MLT, and/or 5 μmol/L Cpd C 2HCl. (a) Flow cytometry was used to detect HK-2 cell apoptosis. (b) Immunofluorescence of Mito-Tracker Red CMXRos-staining (red) (200× magnification) to determine HK-2 cell mitochondrial membrane potential of the respective groups, (c) Immunofluorescence of JC-1 (200× magnification) to determine HK-2 cell mitochondrial membrane potential in the respective groups, (d) ELISA showing caspase-3 activity. Stronger red fluorescence signal correlates with higher mitochondrial membrane potential. Data are presented as the mean ± SEM from three independent experiments. *P < 0.05, **P < 0.01, ***P < 0.001, ****P < 0.0001 versus the NC group; #P < 0.05, ##P < 0.01, ###P < 0.001, ####P < 0.0001 versus the Ox group; ^P < 0.05, ^^P < 0.01, ^^^P < 0.001, ^^^^P < 0.0001 versus the Ox + MLT group.

melatonin's effects on cell viability involve AMPK activation in HK-2 cells.

Melatonin-mediated inhibition of ER stress is partly dependent on AMPK activation

We performed western blot and immunofluorescence analyzes to clarify the role and importance of AMPK activation on melatonin-mediated inhibition of ER stress. Compared with the Ox + MLT group, the Ox + MLT + Cpd C 2HCl group showed increased protein expression of GRP78, DDIT3, ATF6, p-PERK/PERK, p-IRE1/IRE1, XBP1s, caspase-12, cleaved caspase-3, and cleaved caspase-9 in western blot analysis (Figure 6(a)). Increased protein expression of GRP78, ATF6, DDIT3, p-PERK, and p-IRE1 in the Ox + MLT + Cpd C 2HCl group was also confirmed by immunofluorescence (Figure 6(bf)). These results suggest that Compound C 2HCl does not completely inhibit the expression of ER stress and apoptotic proteins, and that the protective effect of melatonin on HK-2 cells is partly dependent on AMPK activation.

Discussion

Kidney stone formation is a complex process, involving super-saturation of urinary lithogenic factors, damage of renal tubular epithelial cells, adhesion, aggregation, nucleation, and growth of crystals [28]. Oxalate is an important component of urinary lithogenic factors. High concentrations of oxalate deposition can lead to oxidative and ER stress damage of renal tubular epithelial cells, thus promoting kidney stone formation [28,29]. We showed in this study that melatonin can regulate the ER stress response mechanism by increasing the antioxidant capacity of HK-2 cells, reducing apoptosis, and maintaining the mitochondrial membrane potential upon oxalate-induced damage. These results indicate that melatonin reduces oxalate-induced oxidative and ER stress damage, potentially inhibiting kidney stone formation. Moreover, our results revealed that the protective effects of melatonin on oxalate-induced ER stress are mediated by AMPK activation.

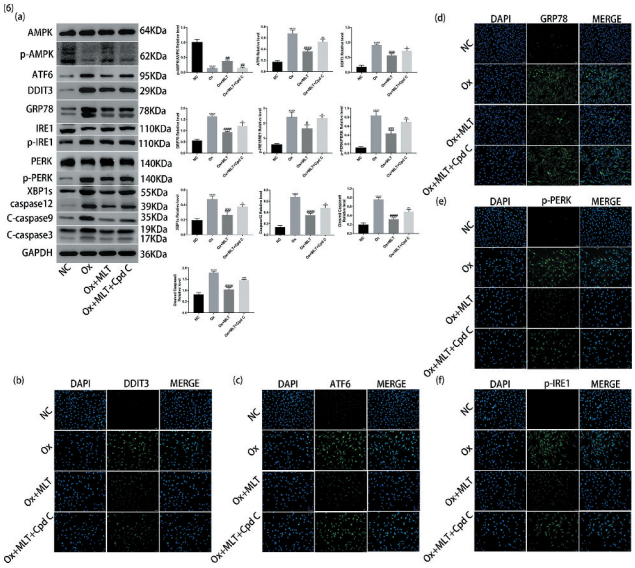

Figure 6. Role of AMPK activation on melatonin-mediated inhibition of ER stress. Cells in each group were treated for 12 h with 4 mmol/L Ox, 10 μmol/L MLT, and/or 5 μmol/L Cpd C 2HCl. (a) Western blot and corresponding histograms of DDIT3, GRP78, ATF6, PERK, p-PERK, IRE1, p-IRE1, XBP1s, caspase-12, cleaved caspase-3, cleaved caspase-9, p-AMPK, and AMPK protein expression relative to GAPDH. Immunofluorescence detection of (b) DDIT3, (c) ATF6, (d) GRP78, (e) p-PERK and (f) p-IRE1 protein expression (200× magnification). Anti-rabbit IgG (H + L), F (ab') 2 Fragment (Alexa Fluor® 488 Conjugate) output green fluorescence. Data are presented as the mean ± SEM from three independent experiments. *P < 0.05, **P < 0.01, ***P < 0.001, ****P < 0.0001 versus the NC group; #P < 0.05, ##P < 0.01, ###P < 0.001, ####P < 0.0001 versus the Ox group; ^P < 0.05, ^^P < 0.01, ^^^P < 0.001, ^^^^P < 0.0001 versus the Ox + MLT group; ns: not significant.

The accumulation of high concentrations of oxalate in renal tubular epithelial cells is due to a dysfunction of intracellular antioxidant mechanisms. This leads to a decrease in endogenous antioxidant enzymes [30], such as SOD, CAT, and GSH, as well as an increase in lipid peroxides [10], such as MDA, ketones, and hydroxyl radicals. When the levels of endogenous antioxidants fall, ROS levels rise, leading to oxidative stress characterized by a decrease in mitochondrial membrane potential [31–33] and oxidative damage to cellular components, such as lipids, nucleic acids, proteins, and DNA [34]. Antioxidants, like melatonin, can protect against oxalate-induced toxicity and promote cell survival by protecting intracellular structures, preventing DNA damage, maintaining redox balance, scavenging free radicals, reducing peroxide levels, and inhibiting lipid peroxidation [14,35]. Indeed, we showed in our study that melatonin treatment significantly increased SOD, CAT, GSH, and T-AOC and significantly decreased MDA levels, affirming the role of melatonin as an endogenous antioxidant. Reduction in ROS and LDH levels, and an increase in HK-2 cell viability after melatonin treatment, supports the function of melatonin as an effective scavenger of oxygen free radicals, as well as its roles in reducing oxalate-induced oxidative stress and cellular toxicity.

The ER stress response is characterized by morphological changes, blocked protein processing and transport, and accumulation of unfolded or misfolded proteins in the ER [36]. Cells subjected to certain stimuli will develop ER stress, and under normal circumstances, cells can relieve ER stress and promote functional recovery through the unfolded protein response (UPR). However, over-stimulation, either in concentration or duration, will cause cell damage and apoptosis [37]. The UPR is mediated by glucose-regulated protein 78 (GRP78) and three stress receptor proteins (ATF6, IRE1, and PERK) [27]. Excessive oxalate deposition can lead to ER stress [38] and disrupt protein folding in the ER. We examined the effects of melatonin on the three branches of the UPR to determine the effect of melatonin on oxalate-induced ER stress. ER stress triggers the dissociation of GRP78 from PERK, an ER type I transmembrane protein, leading to PERK phosphorylation, which in turn induces ATF4 transcription and activation; activated ATF4 then induces the transcription and expression of CHOP [39]. We observed increased p-PERK protein expression, as well as as CHOP protein expression and mRNA levels, in HK-2 cells treated with a high concentration of oxalate for 12 hours. Melatonin treatment significantly reduced PERK activation in these cells. After dissociation from GRP78, IRE1 is activated by dimerization and auto-phosphorylation, and can then induce XBP1u mRNA (uncut XBP1 mRNA) shearing to produce XBP1s mRNA (sheared XBP1 mRNA), a key transcription factor that upregulates UPR-related gene transcription and protein expression [40]. In the present study, we found that oxalate treatment induced IRE1 phosphorylation in HK-2 cells and upregulated XBP1s mRNA levels compared with the control group,

while low p-IRE1 levels were observed in melatonin-treated cells. Accumulation of misfolded proteins in the ER induces the dissociation of the molecular chaperone GRP78 from ATF6 (type II transmembrane glycoprotein), thereby allowing for activated ATF6 to cleave fragments in the nucleus and bind to ER stress response elements; this in turn feeds back and initiates the transcription of GRP78, XBP1, and the ER-related degradation component CHOP [41–43]. ER stress can also activate the zymogen caspase-12 [44], which can act together with CHOP to induce caspase-dependent apoptosis. Therefore, we measured the protein expression and mRNA levels of GRP78, CHOP, and ATF6, and found that high oxalate concentrations correlated with significantly increased mRNA levels and protein expression of ER stress-related factors (GRP78, DDIT3, and ATF6), which was consistent with previous studies [7]. Moreover, we found that melatonin can dose-dependently reduce the levels of GRP78, DDIT3, ATF6, caspase-12, cleaved caspase-3, and cleaved caspase-9 in HK-2 cells. This indicates that ER stress could induce changes in subsequent caspase-dependent apoptosis. Taken together, these findings suggest that melatonin potentially modulates the three branches of the UPR and may prevent oxalate–induced ER stress.

AMPK is generally regarded as an important enzyme in stress responses. It has been shown that AMPK inhibition aggravates ER stress [45,46]. As a cellular energy sensor, AMPK regulates metabolism by controlling the phosphorylation of key energy proteins and transcription factors, promoting glucose and fatty acid uptake, enhancing mitochondrial function and fatty acid oxidation, and inhibiting lipid and cholesterol synthesis [47]. Studies have shown that melatonin can reduce vascular calcification through AMPK activation [17] and can prevent alcohol-induced liver damage [16]. Melatonin reportedly can alleviate ER stress in hypoxia-reoxygenation injury of N2a neuroblastoma cells by activating the AMPK-Pak2 pathway [23]. Moreover, the melatonin-MTNR1A system reportedly regulates the level of cAMP in renal tubular epithelial cells and modulates the binding and internalization of calcium oxalate crystals [48], which can promote kidney stone formation [49]. Thus, we speculate that melatonin can increase intracellular cAMP levels by activating AMPK, thereby inhibiting the binding and internalization of oxalate crystals and reducing ER stress and toxicity. In the present study, we found that p-AMPK levels were reduced in oxalate-treated HK-2 cells, and that melatonin restored the p-AMPK levels. These findings indicate that melatonin can induce AMPK activation. Thus, we used Compound C 2HCl, a reported AMPK inhibitor, to clarify the association between melatonin and AMPK activation. Interestingly, the addition of Compound C 2HCl decreased the mitochondrial membrane potential, increased the expression of ER stress-related and apoptotic proteins, and reduced cell apoptosis. The Compound C 2HCl-mediated reversal of the effects of melatonin in HK-2 cells indicates that melatonin acts via the AMPK pathway to modulate ER-stress.

Although we did not use transmission electron microscopy to monitor changes in the ER and its contents in this study, we showed the protective effect of melatonin against oxalate-induced ER stress and apoptosis in HK-2 cells using flow cytometry, ELISA, immunofluorescence, RT-PCR, and western blot analyzes. Our results also suggest that melatonin's protective effects against oxalate-induced ER stress involve the AMPK signaling pathway. This study is the first to show that melatonin protects against oxalate toxicity, suggesting that melatonin could be potentially used in the prevention and treatment of oxalate-mediated renal injury and the formation of kidney stones.

Data availability statement

The original data is available upon reasonable request.

Disclosure statement

The authors declare that they have no conflicts of interest.

Funding

This work was supported by the National Natural Science Foundation of China [31600785].

References

[1] Khan SR, Pearle MS, Robertson WG, et al. Kidney stones[J]. Nat Rev Dis Primers. 2016;2(1):16008.

[2] Corbo J, Wang J. Kidney and ureteral stones. Emerg Med Clin North Am. 2019;37(4):637–648.

[3] Scales CD Jr., Smith AC, Hanley JM, et al. Prevalence of kidney stones in the United States[J]. Eur Urol. 2012;62(1):160–165.

[4] Yang SX, Song C, Xiong YH. Current perspectives on urolithiasis management in China[J]. World J Urol. 2019. DOI:10.1007/s00345-019-03026-9.

[5] Kaufman DW, Kelly JP, Curhan GC, et al. Oxalobacter formigenes may reduce the risk of calcium oxalate kidney stones[J]. J Am Soc Nephrol. 2008;19 (6):1197–1203.

[6] Khan SR. Renal tubular damage/dysfunction: key to the formation of kidney stones[J]. Urol Res. 2006;34 (2):86–91.

[7] Kang J, Sun Y, Deng Y, et al. Autophagy-endoplasmic reticulum stress inhibition mechanism of superoxide dismutase in the formation of calcium oxalate kidney stones[J]. Biomed Pharmacother. 2020;121:109649.

[8] Khan SR. Reactive oxygen species as the molecular modulators of calcium oxalate kidney stone formation: evidence from clinical and experimental investigations[J]. J Urol. 2013;189(3):803–811.

[9] Thamilselvan V, Menon M, Thamilselvan S. Selective Rac1 inhibition protects renal tubular epithelial cells from oxalate-induced NADPH oxidase-mediated oxidative cell injury[J]. Urol Res. 2012;40(4):415–423.

[10] Cao LC, Honeyman TW, Cooney R, et al. Mitochondrial dysfunction is a primary event in renal cell oxalate toxicity[J]. Kidney Int. 2004;66 (5):1890–1900.

[11] Acuna-Castroviejo D, Escames G, Venegas C, et al. Extrapineal melatonin: sources, regulation, and potential functions[J]. Cell Mol Life Sci. 2014;71 (16):2997–3025.

[12] Stacchiotti A, Favero G, Rodella LF. Impact of melatonin on skeletal muscle and exercise. Cells. 2020;9(2):2.

[13] Cipolla-Neto J, Amaral FGD. Melatonin as a hormone: new physiological and clinical insights. Endocr Rev. 2018;39(6):990–1028.

[14] Rodriguez C, Mayo JC, Sainz RM, et al. Regulation of antioxidant enzymes: a significant role for melatonin. J Pineal Res. 2004;36(1):1–9.

[15] Sener TE, Sener G, Cevik O, et al. The effects of melatonin on ethylene glycol-induced nephrolithiasis: role on osteopontin mRNA gene expression. Urology. 2017;99:287 e289–287 e215.

[16] Rui BB, Chen H, Jang L, et al. Melatonin upregulates the activity of AMPK and attenuates lipid accumulation in alcohol-induced rats. Alcohol Alcohol. 2016;51 (1):11–19.

[17] Chen WR, Yang JQ, Liu F, et al. Melatonin attenuates vascular calcification by activating autophagy via an AMPK/mTOR/ULK1 signaling pathway[J]. Exp Cell Res. 2020;111883. DOI:10.1016/j.yexcr.2020.111883.

[18] Qi D, Young LH. AMPK: energy sensor and survival mechanism in the ischemic heart[J]. Trends Endocrinol Metab. 2015;26(8):422–429.

[19] Ramesh M, Vepuri SB, Oosthuizen F, et al. Adenosine monophosphate-activated protein kinase (AMPK) as a diverse therapeutic target: a computational perspective. Appl Biochem Biotechnol. 2016;178 (4):810–830.

[20] Mihaylova MM, Shaw RJ. The AMPK signalling pathway coordinates cell growth, autophagy and metabolism[J]. Nat Cell Biol. 2011;13(9):1016–1023.

[21] Amin R, Sharma S, Ratakonda S, et al. Extracellular nucleotides inhibit oxalate transport by human intestinal Caco-2-BBe cells through PKC-delta activation[J]. Am J Physiol Cell Physiol. 2013;305(1):C78–89.

[22] Bhargava P, Schnellmann RG. Mitochondrial energetics in the kidney. Nat Rev Nephrol. 2017;13 (10):629–646.

[23] Xing J, Xu H, Liu C, et al. Melatonin ameliorates endoplasmic reticulum stress in N2a neuroblastoma cell hypoxia-reoxygenation injury by activating the AMPK-Pak2 pathway. Cell Stress Chaperones. 2019;24(3):621–633.

[24] Bae HR, Kim DH, Park MH, et al. beta-Hydroxybutyrate suppresses inflammasome formation by ameliorating endoplasmic reticulum stress via AMPK activation. Oncotarget. 2016;7 (41):66444–66454.

[25] Modrzynski JJ, Christensen JH, Brandt KK. Evaluation of dimethyl sulfoxide (DMSO) as a co-solvent for toxicity testing of hydrophobic organic compounds. Ecotoxicology. 2019;28(9):1136–1141.

[26] Zhou G, Myers R, Li Y, et al. Role of AMP-activated protein kinase in mechanism of metformin action. J Clin Invest. 2001;108(8):1167–1174.

[27] Iurlaro R, Munoz-Pinedo C. Cell death induced by endoplasmic reticulum stress. Febs J. 2016;283 (14):2640–2652.

[28] Tsujihata M. Mechanism of calcium oxalate renal stone formation and renal tubular cell injury. Int J Urol. 2008;15(2):115–120.

[29] Khan SR, Shevock PN, Hackett RL. Acute hyperoxaluria, renal injury and calcium oxalate urolithiasis. J Urol. 1992;147(1):226–230.

[30] Khand FD, Gordge MP, Robertson WG, et al. Mitochondrial superoxide production during oxalate-mediated oxidative stress in renal epithelial cells. Free Radic Biol Med. 2002;32(12):1339–1350.

[31] Joshi S, Peck AB, Khan SR, Peck AB, Khan SR. NADPH oxidase as a therapeutic target for oxalate induced injury in kidneys. Oxid Med Cell Longev. 2013;2013:462361.

[32] Joshi S, Saylor BT, Wang W, et al. Apocynin-treatment reverses hyperoxaluria induced changes in NADPH oxidase system expression in rat kidneys:

a transcriptional study[J]. PLoS One. 2012;7(10): e47738.
[33] Zuo J, Khan A, Glenton PA, et al. Effect of NADPH oxidase inhibition on the expression of kidney injury molecule and calcium oxalate crystal deposition in hydroxy-L-proline-induced hyperoxaluria in the male Sprague-Dawley rats. Nephrol Dial Transplant. 2011;26 (6):1785–1796.
[34] Liu Y, Li D, He Z, et al. Inhibition of autophagy-attenuated calcium oxalate crystal-induced renal tubular epithelial cell injury in vivo and in vitro. Oncotarget. 2018;9(4):4571–4582.
[35] Ali T, Rehman SU, Shah FA, et al. Acute dose of melatonin via Nrf2 dependently prevents acute ethanol-induced neurotoxicity in the developing rodent brain. J Neuroinflammation. 2018;15(1):119.
[36] Reyes-Fermin LM, Aparicio-Trejo OE, Avila-Rojas SH, et al. Natural antioxidants' effects on endoplasmic reticulum stress-related diseases. Food Chem Toxicol. 2020;138:111229.
[37] Oakes SA, Papa FR. The role of endoplasmic reticulum stress in human pathology. Annu Rev Pathol. 2015;10:173–194.
[38] Sun Y, Kang J, Tao Z, et al. Effect of endoplasmic reticulum stress-mediated excessive autophagy on apoptosis and formation of kidney stones. Life Sci. 2020;244:117232.
[39] Yi S, Chen K, Zhang L, et al. Endoplasmic reticulum stress is involved in stress-induced hypothalamic neuronal injury in rats via the PERK-ATF4-CHOP and IRE1-ASK1-JNK pathways. Front Cell Neurosci. 2019;13:190.
[40] Chalmers F, van Lith M, Sweeney B, et al. Inhibition of IRE1alpha-mediated XBP1 mRNA cleavage by XBP1 reveals a novel regulatory process during the unfolded protein response. Wellcome Open Res. 2017;2:36.
[41] Shore GC, Papa FR, Oakes SA. Signaling cell death from the endoplasmic reticulum stress response. Curr Opin Cell Biol. 2011;23(2):143–149.
[42] Hillary RF, FitzGerald U. A lifetime of stress: ATF6 in development and homeostasis. J Biomed Sci. 2018;25 (1):48.
[43] Yoshida H, Matsui T, Yamamoto A, et al. XBP1 mRNA is induced by ATF6 and spliced by IRE1 in response to ER stress to produce a highly active transcription factor. Cell. 2001;107(7):881–891.
[44] Szegezdi E, Fitzgerald U, Samali A. Caspase-12 and ER-stress-mediated apoptosis: the story so far. Ann N Y Acad Sci. 2003;1010(1):186–194.
[45] Boss M, Newbatt Y, Gupta S, et al. AMPK-independent inhibition of human macrophage ER stress response by AICAR. Sci Rep. 2016;6(1):32111.
[46] Tong JF, Yan X, Zhu MJ, et al. AMP-activated protein kinase enhances the expression of muscle-specific ubiquitin ligases despite its activation of IGF-1/Akt signaling in C2C12 myotubes. J Cell Biochem. 2009;108(2):458–468.
[47] Desjardins EM, Steinberg GR. Emerging role of AMPK in brown and beige adipose tissue (BAT): implications for obesity, insulin resistance, and type 2 diabetes. Curr Diab Rep. 2018;18(10):80.
[48] Esposito T, Rendina D, Aloia A, et al. The melatonin receptor 1A (MTNR1A) gene is associated with recurrent and idiopathic calcium nephrolithiasis. Nephrol Dial Transplant. 2012;27(1):210–218.
[49] Lieske JC. Huang E and Toback F G. Regulation of renal epithelial cell affinity for calcium oxalate monohydrate crystals. Am J Physiol Renal Physiol. 2000;278 (1):F130–137.